

Research Article

Traction Control System for Motorcycles

Pascal Cardinale, Camillo D'Angelo, and Massimo Conti

*Dipartimento di Ingegneria Biomedica, Elettronica e Telecomunicazioni, Università Politecnica delle Marche,
Via Brecce Bianche, 60121 Ancona, Italy*

Correspondence should be addressed to Massimo Conti, m.conti@univpm.it

Received 31 August 2008; Accepted 23 October 2008

Recommended by Markus Kucera

Traction control is a widely used control system to increase stability and safety of four wheel vehicles. Automatic stability control is used in the BMW K1200R motorcycle and in motoGP competition, but not in other motorcycles. This paper presents an algorithm and a low-cost real-time hardware implementation for motorcycles. A prototype has been developed, applied on a commercial motorcycle, and tested in a real track. The control system that can be tuned by the driver during the race has been appreciated by the test driver.

Copyright © 2009 Pascal Cardinale et al. This is an open access article distributed under the Creative Commons Attribution License, which permits unrestricted use, distribution, and reproduction in any medium, provided the original work is properly cited.

1. Introduction

Traction control is a widely used control system in automotive applications to increase stability and safety of vehicles. Well-known vehicle control systems such as antilock brake system (ABS), antiSlip regulation (ASR), and electronic stability program (ESP) are used in internal combustion engine vehicles (ICVs).

Traction control prevents the vehicle from swerving when accelerating on a loose surface, reduces engine output until the vehicle can move without the wheels skidding, and produces maximum stability when cornering especially in wet or icy roads.

A conventional differential does not usefully distribute the torque to the wheels when a wheel is skidding. All the power is applied to the skidding wheel and not to the wheel that has more traction. An electronic traction control system prevents a wheel from skidding by applying a brake to that wheel, enabling the differential to apply power to the other wheel.

The control scheme is composed by a device that estimates the road surface condition and a traction controller that regulates the wheel slip at desired values. Several control strategies have been proposed in the literature mainly based on sliding mode controllers, fuzzy logic, and adaptive schemes to control four wheels vehicles moving in sliding

surface [1–8]. Such control schemes are motivated by the fact that the system is nonlinear and uncertain.

Recently, a lot of work in the definition of traction control algorithms for electric vehicles (EV) has been developed [9–15]. In EV, the torque generation is very quick and accurate, both for accelerating and decelerating. The torque control of each wheel is ensured by the inverter, and it does not require a mechanical differential gear. The electronic control of the torque and of the speed of each one of the four independent wheels allows the EV to operate more efficiently avoiding slippage. Furthermore, an efficient control of the torque allows an increment of the energy efficiency of the vehicle.

The application of traction control to motorcycles is not so widely used as to four wheel vehicles, probably because of the high cost of the control system.

BMW and Kawasaki were the first companies that applied ABS to motorcycles. BMW is the unique company that is using an automatic stability control (ASC) system in top high-torque BMW K1200R commercial model from 2007. BMW ASC prevents the rear wheel from skidding uncontrolled when accelerating, and thus it avoids any loss of side forces and stability [16, 17].

Additional sensors have been inserted to the BMW K1200R motorcycle in order to determine the speed at which each wheel is turning, as shown in Figure 1. A high number

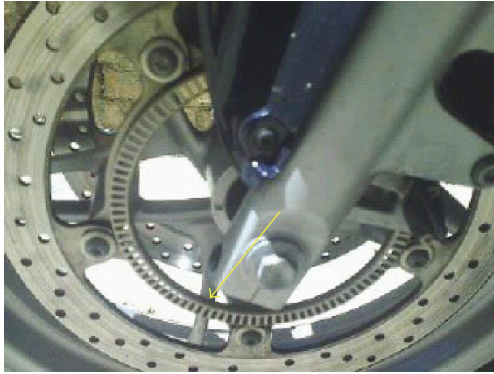


FIGURE 1: Particular of BMW K1200R.

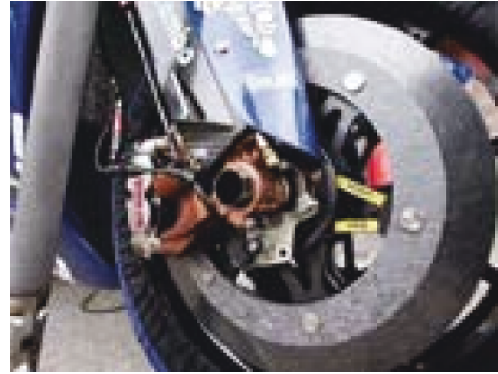


FIGURE 3: Hall sensor and bolts in the MotoGP Yamaha M1.

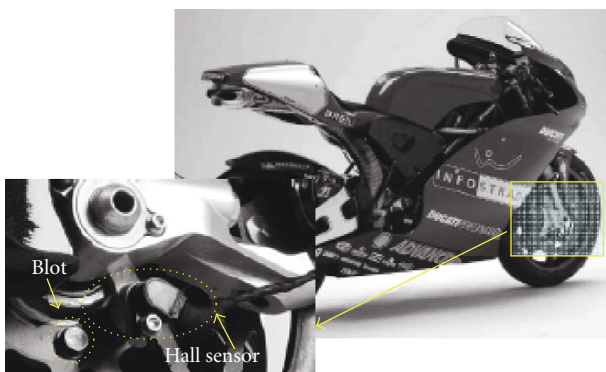


FIGURE 2: Hall sensor and bolts in the MotoGP Ducati racing.

of pick-up points for the wheel speed sensor give a high resolution to the data, enabling a traction control system to react faster. The BMW K1200R uses about 100 pick-up points in the wheel, the holes evidenced by the arrow in the particular of Figure 1, in order to have an accurate precision in the speed estimation required for the ABS, and the same information is used by the ASC system.

Registering any sudden change in the difference in speed front-to-rear, the electronic control unit is able to detect any risk of the rear wheel skidding, engine management responding immediately by intervening in the ignition angle to take back engine power [16, 17].

Traction control systems are used in motoGP (e.g., Yamaha and Ducati), to improve the ability in driving the motorcycle during competitions [18]. In Ducati motoGP, the wheel speed is measured using hall effect gear tooth sensors, see Figure 2, in a way similar to the one used in this work. The Ducati motoGP uses 8 pick-up points (the bolts).

The motoGP Yamaha M1 has sensors on each side of the wheel, for redundancy. The solid disc used, as shown in Figure 3, is a magnetic ring element, into which a strip of small magnets is embedded for more data points and accuracy than a toothed ring.

The details on the traction control systems used in motoGP and by BMW, in our knowledge, are not available. Traction control systems are not used in other commercial motorcycles or in supermotard or motocross motorcycles.

This paper presents a new algorithm and its hardware implementation on low-cost real-time embedded system implementing traction control for supermotard or motocross motorcycles. A key innovative feature, proposed in this work, is that the control of the torque is obtained introducing a cut in the ignition spark using a switch in parallel to the switch used to turn off the engine. Therefore, the torque control is obtained without modifying the ignition controller and it can be applied to every existing commercial motorcycle.

Furthermore, supermotard or motocross motorcycles do not move always on asphalt, and the condition of the ground can change very rapidly. Therefore, the driver must tune the traction control on the fly.

Therefore, the driver must tune the traction control on the fly. This is allowed by the algorithm and architecture proposed in this work.

Section 2 reports a brief description of problems related to the traction control of motorcycles. The proposed architecture, the control algorithm, and the performance analysis of the system are presented in Section 3. Section 4 reports some experimental results obtained in a race track.

2. Traction Control for Motorcycles

Critical conditions in driving a motorcycle are the rearing up or when the motorcycle is in bend. The objective of the proposed control system is to help the driver in maintaining a secure control of the motorcycle in rearing up and in bend. In both cases, the excessive torque of the engine on the rear wheel may cause the loss of control of the motorcycle.

Figure 4 shows an example of a rearing up, it happens when the motorcycle is not in bend and the torque is too high. In this case, the speed of the rear wheel is greater than the speed of the front wheel.

The driver can avoid rearing up, reducing the opening of the butterfly valve controlling the accelerator.

Figure 5 shows an example of a motorcycle in a critical situation in bend. In this case, the front wheel is closer to the centre of the bend with respect to the rear wheel that is going faster and more and more far from the centre of the bend. In this situation, the driver can lose the control of the



FIGURE 4: Rearing up.



FIGURE 5: Motorcycle in bend.

motorcycle. To avoid this, the driver should reduce the torque in order to reduce the speed of the rear wheel.

In both cases, the objective of the traction control is to reduce the torque on the rear wheel in order to keep equal the speed of the two wheels. To do this, an estimation of the speed of both the wheels must be performed using specific sensors.

3. Traction Controller Architecture

The main specification of the proposed system is its simple applicability to existing motorcycle independently on the different ignition control system.

The torque applied to the rear wheel can be controlled reducing the gasoline injected closing the butterfly valve or reducing the electrical current to the sparking plug. The former cannot be easily obtained without changing the injection controller, while the latter has been simply obtained, as it will be shown in this section.

Figure 6 shows a general scheme that gives the electrical current to the sparking plug. Every motorcycle has a manual switch used to turn off the engine; the switch simply bypasses to ground the electrical current flowing in the sparking coil. The proposed system modifies the sparking scheme inserting an additional switch in parallel to the manual turn off switch.

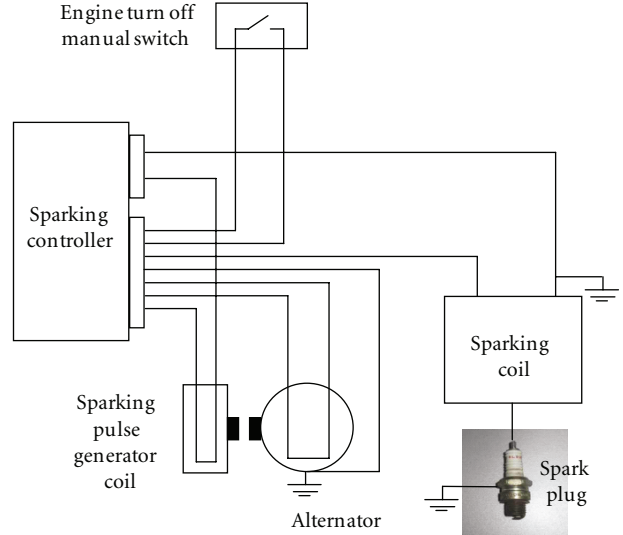


FIGURE 6: General scheme of a sparking controller.

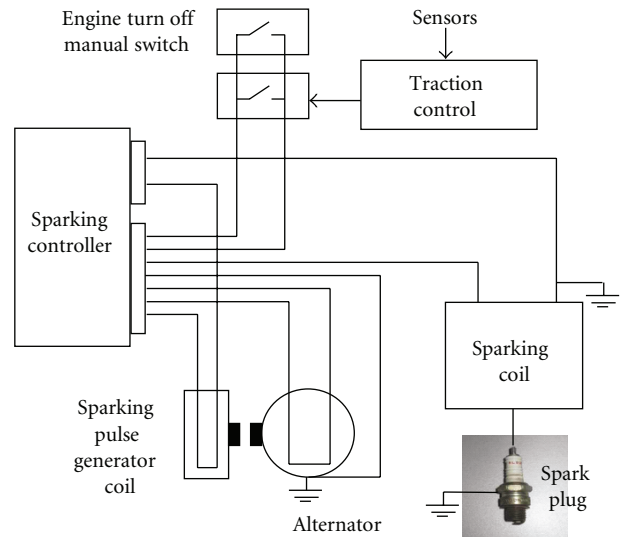


FIGURE 7: Proposed modification of sparking controller with traction control.

This switch is controlled by a microcontroller on the basis of the output of some additional sensors, as shown in Figure 7.

The effect of the traction controller is shown in Figure 8. In the top of the figure, the voltage applied to the spark plug during a normal sparking is reported, in the bottom, a cut in the pulse, introduced by the traction controller, can be seen.

The cut on the electrical current of the spark plug is obtained in two ways: defining the cut-off delay between the start of the ignition spark and the intervention of the traction control, as shown in Figure 8, and defining the number of consecutive ignition sparks for which the traction control takes action, an example is shown in Figure 9. The ignition spark cut off, imposed by the traction controller, modifies the torque applied to the wheel.

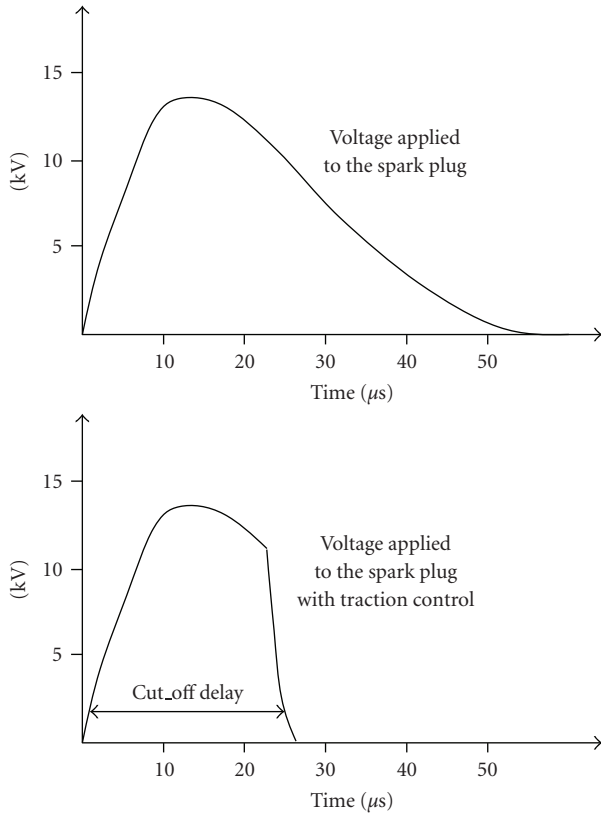


FIGURE 8: Voltage applied to the sparking plug (top) without traction control and (bottom) with traction control.

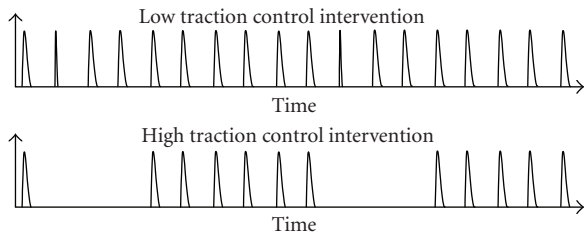


FIGURE 9: Examples of low and high traction control intervention on the ignition spark.

The complete architecture of the traction control system is reported in Figure 10.

The core of the control algorithm is implemented in a 40 MHz Microchip PIC18F6527 microcontroller.

Six sensors are added to give information on the situation of the motorcycle to the controller: front wheel speed sensor, rear wheel speed sensor, sparking signal, rolling angle sensor, butterfly valve opening sensor, and engine r.p.m. sensor. The driver can modify the parameters of the controller pushing few buttons even driving the motorcycle. The microcontroller stores information on a 1 Mbyte flash memory with the purpose of monitoring the performances of the control system. A display is placed in the motorcycle to allow the driver to verify in real time the status of the

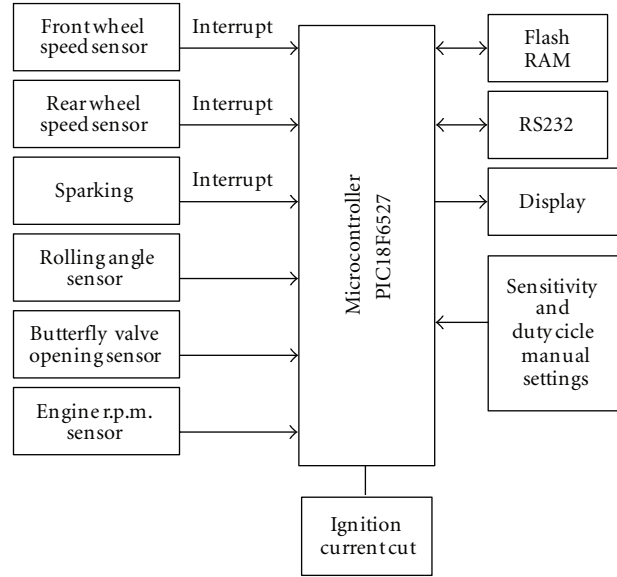


FIGURE 10: Architecture of the traction controller.

controller. An RS232 interface is used to communicate with an external PC when the motorcycle is parking.

3.1. Wheel Speed Sensors. The wheel speed is measured using hall effect gear tooth sensors. The sensor output voltage is 5 V when the sensor is in proximity to a ferromagnetic material, otherwise the output voltage is 0.2 V. The hall sensor is placed close to the 4 ferromagnetic bolts of the wheel of our motorcycle, as shown in Figure 11. During wheel rotation, the sensor sends a pulse when the bolt is close to the sensor. The time interval between two pulses is inversely proportional to the angular speed of the wheel. The wheel speed is estimated knowing the time interval between the pulses, the effective diameter of the tyre, and the number of bolts in each wheel. Figure 11 shows the sensor applied to the front and rear wheels in our prototype.

The same principle is applied in the BMW K1200R.

3.2. Rolling Angle Sensors. The wheel speed estimation depends on the rolling angle of the motorcycle and other parameters like tyre, pressure, and temperature. Figure 12 shows the effect of the rolling angle on the effective tyre diameter. An increment in the rolling angle causes a reduction of the effective diameter of the wheel and therefore a reduction in the wheel speed.

The difference between the nominal and effective tyre diameter in bend can be higher than 10% considering that the motorcycle in bend can have a rolling angle higher than 60° and the distortion of the part of the wheel that touches the ground during the bend. Furthermore, this difference depends on the tyre pressure, temperature, and consumption. The error on the wheel speed estimation due to this effect is not negligible, therefore, a rolling sensor of the VTI technologies has been inserted and the information are used in the algorithm for the wheel speed estimation.

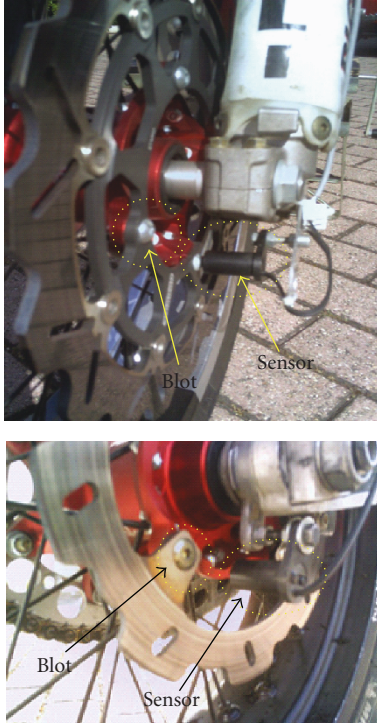


FIGURE 11: Hall sensor and one of the bolt in the front and rear wheels.

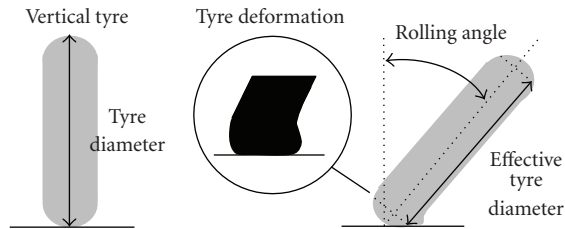


FIGURE 12: Dependence of the rolling angle on the effective tyre.

3.3. Butterfly Opening Sensor and Engine r.p.m. Sensor. The opening of the butterfly has been measured with a precision potentiometer of Vishay company connected to the accelerator cable. The r.p.m. of the engine is indispensable to measure the torque and the power of the engine.

3.4. Electrical Current Switch. Different solutions have been studied to obtain a cut in the electric current of the sparking plug. An electromechanic relay of multicomp was not fast enough to obtain a shape similar to the one shown in Figure 8. The solution chosen is an IGBT.

3.5. Microcontroller and Control Algorithm. The control algorithm used is shown in Figure 13. The parameter settings are stored in the memory, but they can be modified by the driver during the race using push-buttons to increment or decrement the values of ε and δ . The parameter δ is

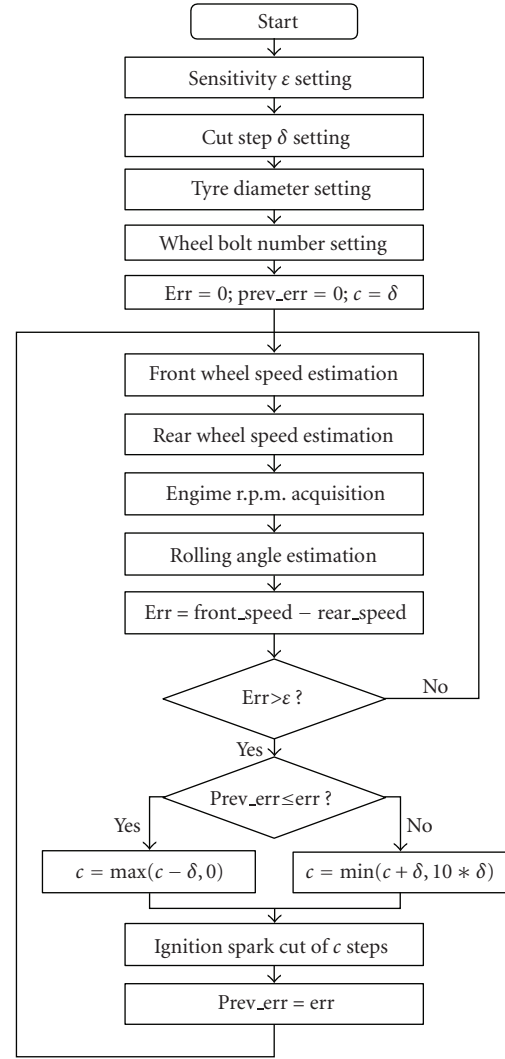


FIGURE 13: Control algorithm implemented in the microcontroller.

the minimum increment or decrement of the cut_off delay represented in Figure 8. When the ignition cut c is higher than a fixed value, the ignition spark is completely eliminated and the width of the successive ignition spark is reduced, as shown in Figure 9. The complete elimination up to three successive sparks does not have effect on the driving, as it has been verified by experimental results in a real track.

The parameter ε defines the value of difference between front wheel speed and rear wheel speed for which the traction control system takes action. This parameter depends on the driver style of drive and on the ground conditions (asphalt or ground, wet or dry). The front wheel speed and rear wheel speed are estimated, as reported in subsections 3.1 and 3.2, and their difference is used to calculate the width of the cut on the electrical current of the spark plug. When the microcontroller receives an interrupt from the wheel speed sensors, it evaluates if the ignition spark cut must be done and the cut_off delay. When it receives the interrupt from the sparking signal that indicates that the ignition spark started, it eventually waits for a time equivalent to the cut_off

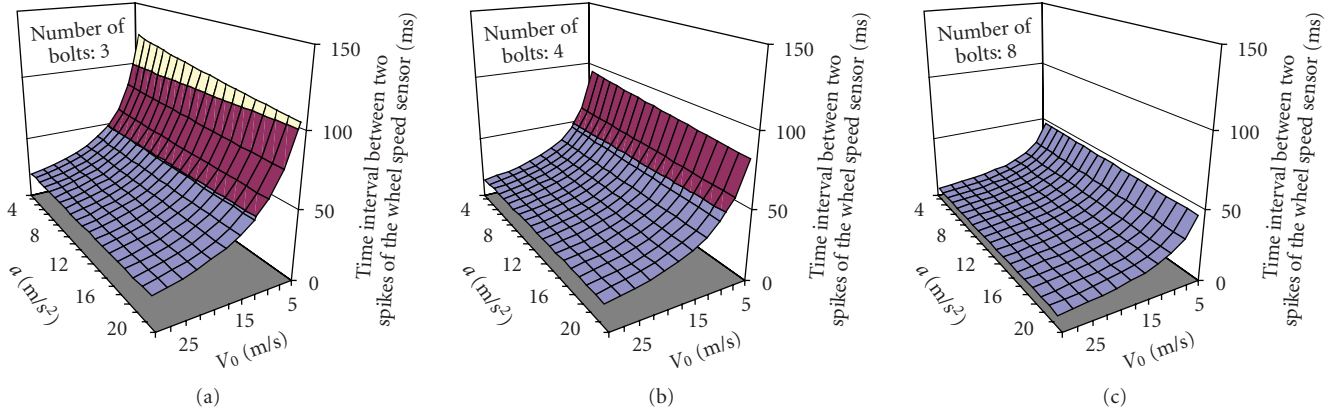


FIGURE 14: Time interval between two spikes of the wheel speed sensor.

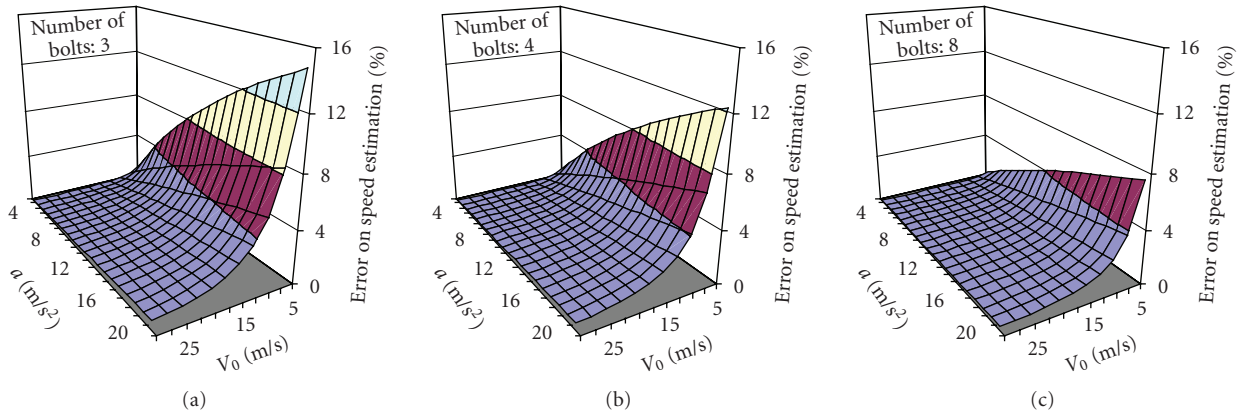


FIGURE 15: Relative error on speed estimation.

delay and operates the ignition spark cut. The algorithm has been translated in assembly code and implemented in the Microchip PIC18F6527 microcontroller with 40 MHz clock, 10 MHz bus clock, and 100 nanoseconds instruction time. The maximum time required to generate the cut has been estimated.

- (i) Front wheel speed estimation 4.7 microseconds
- (ii) Rear wheel speed estimation 4.7 microseconds.
- (iii) Rolling angle estimation 38.0 microseconds.
- (iv) Butterfly opening estimation 10.0 microseconds.
- (v) Engine r.p.m. estimation 4.7 microseconds.
- (vi) Err calculus 118.8 microseconds.
- (vii) Total time 176.7 microseconds.

The time required for the traction control by the microcontroller is, therefore, negligible compared with the minimum time between two consecutive ignition sparks (180 milliseconds for 20000 r.p.m.) and with the average time interval between two pulses coming from the hall sensor used to estimate the wheel speed (about 20 milliseconds for a speed of 20 m/s). Therefore, the digital controller implemented is able to control in real time the traction of the motorcycle.

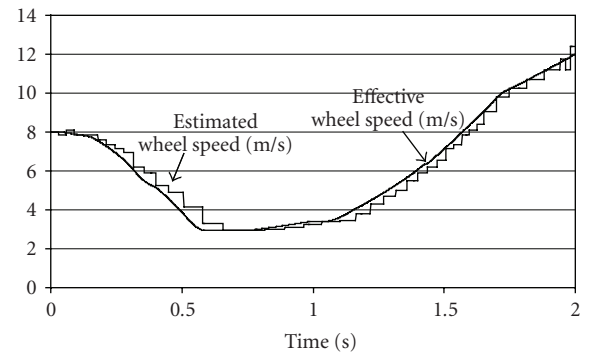


FIGURE 16: Effective and estimated wheel speed in a simulation of a curve with 8 bolts for wheel.

The critical aspect of the traction control system is the number of bolts in each wheel and not the computation time of the microcontroller. The distance Δx covered by the wheel in the time interval Δt between two pulses of the hall effect sensor is

$$\Delta x = \frac{\pi d'}{n}, \quad (1)$$

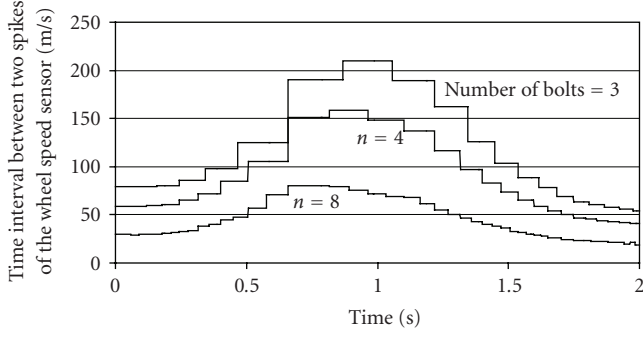


FIGURE 17: Time interval between two spikes of the wheel speed sensor for different number of bolts in the simulation example of Figure 16.

where n is the number of bolts, and d' is the effective diameter of the wheel, considering the rolling angle effect. As an example, let us consider the case of a constant acceleration a starting from an initial speed v_o . In this case, the following relationship is valid:

$$\Delta x = \frac{1}{2}a\Delta t^2 + v_o\Delta t. \quad (2)$$

Therefore, using (1) and (2), it results

$$\Delta t = \sqrt{\frac{v_o^2}{a^2} + 2\frac{\pi d'}{na}} - \frac{v_o}{a}. \quad (3)$$

The value of Δt in (3) is the sampling time of the speed estimate and it is the delay with which the control system knows the wheel speed.

Figure 14 reports the value of Δt in milliseconds as a function of the acceleration and of the velocity v_o for different values of the number of bolts of the wheel for a wheel diameter of 60 cm.

It can be seen that the delay of the control system (177 microseconds) is three-order of magnitude less than Δt .

Conversely Δt is of the same order of magnitude of the time interval between two consecutive ignition sparks, which depends on the engine r.p.m.

A reduction of Δt can be obtained increasing the number of bolts, but this solution is expensive. The BMW K1200R motorcycle uses 100 of pick-up points for wheel speed estimation, while the Ducati motoGP uses 8 pick-up points (the bolts).

The speed estimation v_E performed by the microcontroller is

$$v_E = \frac{\Delta x}{\Delta t}. \quad (4)$$

Using (3), we obtain

$$v_E = \frac{\pi d'/n}{\sqrt{v_o^2/a^2 + 2(\pi d'/na)} - v_o/a}. \quad (5)$$

The maximum relative error between the speed estimation v_E and the effective speed is

$$\Delta v(\%) = \frac{v(\Delta t) - v_E}{v(\Delta t)} 100, \quad (6)$$

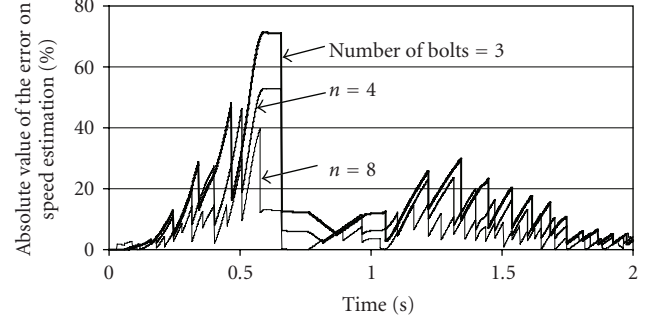


FIGURE 18: Absolute value of the relative error between estimated and effective speed for different number of bolts in the simulation example of Figure 16.



FIGURE 19: Traction control board applied in a supermotard motorcycle.

where

$$v(\Delta t) = \sqrt{v_o^2 + 2a\frac{\pi d'}{n}}. \quad (7)$$

The error is reduced by increasing the number of bolts (4 is the minimum acceptable), it increases for strong acceleration and low values of speed. Figure 15 reports the value of $\Delta v(\%)$ as a function of the acceleration and of the velocity v_o for different values of the number of bolts of the wheel for a wheel diameter of 60 cm. This error depends on speed and acceleration; therefore it reduces the efficiency of the traction control system since it can be only partially compensated by an appropriate tuning of the control parameters.

To verify the error on speed estimation in practical cases, a simple numerical simulator has been developed. Figure 16 reports the effective and estimated wheel speed in a simulation example of a curve with 8 bolts for wheel.

Figure 17 reports the time interval between two spikes of the wheel speed sensor for different number of bolts in the same example, while Figure 18 shows the absolute value of the relative error between estimated and effective speed for different number of bolts.

When the motorcycle is exiting from the curve, the speed is low and the acceleration is high and the error due to a reduced number of bolts is critical.

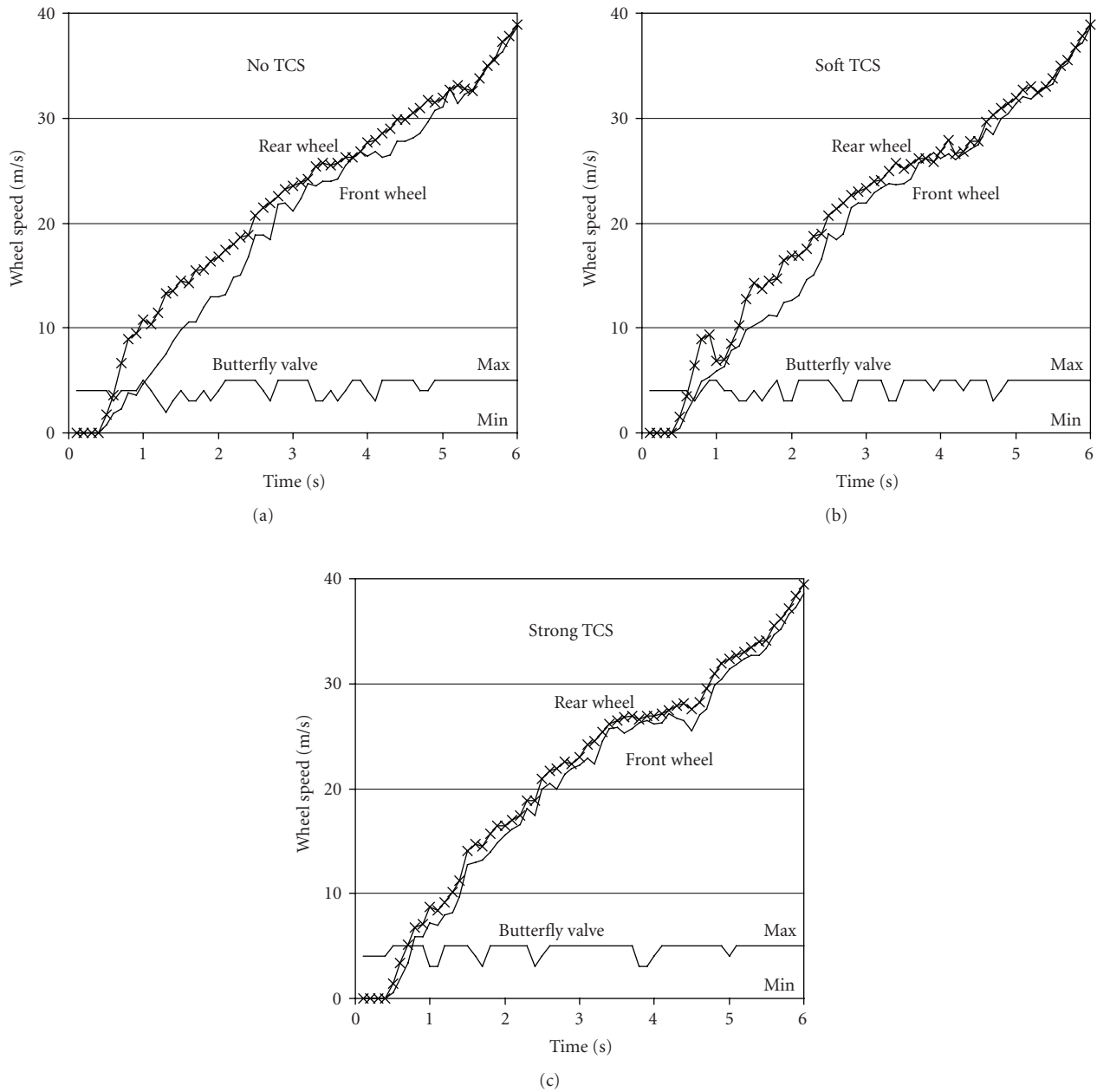


FIGURE 20: Wheel speed and butterfly valve opening for a rearing up test. Without traction control, with traction control “soft control” setting and “strong control” setting.

4. Experimental Results

The system has been implemented and applied to a commercial supermotard motorcycle, shown in Figure 19, in Figure 4, and in Figure 11.

The traction control system has been tested by the authors in the racing track “Enzo e Dino Ferrari” of Fermo, Italy. Some results are shown in this section. The experimental data have been stored in the flash memory during the test in the racing track and then transferred on a PC using the RS232 interface at the end of the race.

The system has also been tested by the Supermoto rider Attilio Pignotti: 2nd in Supermoto S2 World Championship in 2007, 10th in Supermoto S2 World Championship in 2006, and 8th in Supermoto S2 World Championship in 2005.

The results in a rearing up and with the motorcycle in bend are reported in this section.

Figure 20 shows three cases of rearing up starting from 0 m/s to 40 m/s in a straight track, in a situation similar to the photo in Figure 4. With the accelerator in the maximum position, the motorcycle rears up, and the speed of the rear wheel is higher with respect to the front wheel.

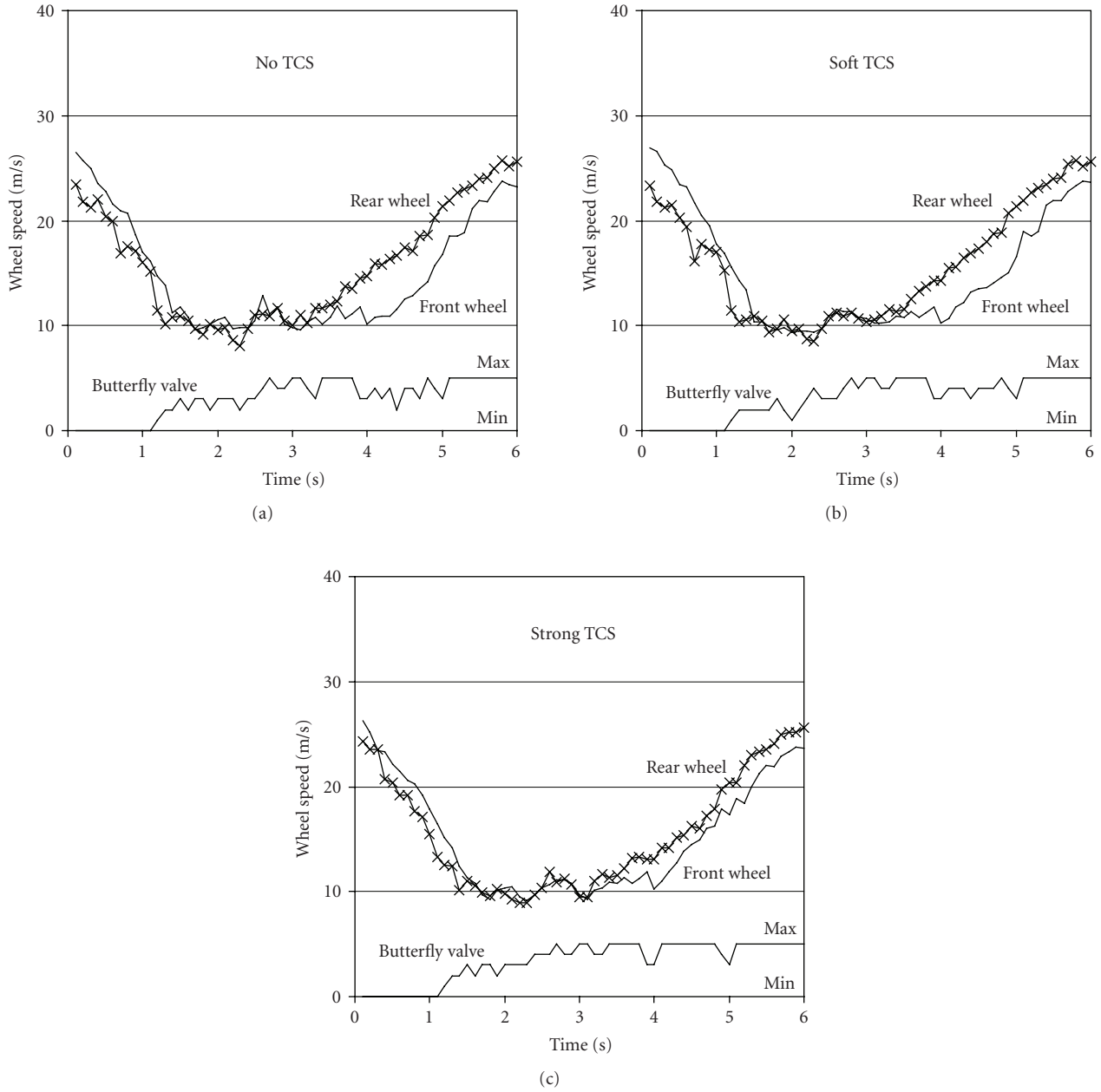


FIGURE 21: Wheel speed, butterfly valve opening, and traction control intervention for a bend test. Without traction control, with traction control “soft control” setting and “strong control” setting.

The same part of the track has been driven through with different traction control strategies.

- (A) NO TCS: without traction control.
- (B) Soft TCS: with traction control with a high value of ϵ , that is the traction control operates only when the difference between the speed of the two wheels is high, giving a “soft control.”
- (C) Strong TCS: with traction control with a low value of ϵ , that is the traction control operates even when the difference between the speed of the two wheels is not too high, giving a “strong control.”

Figure 20 reports the opening of the butterfly controlled by the driver, the intervention of the traction controller, the speed of the front wheel, and the speed of the rear wheel. The effect of the traction control is evident. In case (C), the speed of the front wheel is similar to the speed of the rear wheel and consequently, the motorcycle does not rear up.

Figure 21 shows three cases of a motorcycle in bend, in a situation similar to the photo in Figure 5. In the first part of the bend, the driver reduces the accelerator and uses brakes to reduce the speed. In this case, the front wheel speed is higher with respect to the rear wheel, mainly due to the brake intervention. In the second part of the bend, the driver

accelerates to increase the speed exiting the bend, but if the torque is too high, the rear wheel tends to go in the external part of the bend, as shown in Figure 5, and the rear wheel speed is higher than the front wheel. In this case, the driver may lose the control of the motorcycle.

The same bend has been driven through with different traction control strategies.

- (A) NO TCS: without traction control.
- (B) Soft TCS: with traction control with a high value of ε , that is the traction control operates only when the difference between the speed of the two wheels is high, giving a “soft control.”
- (C) Strong TCS: with traction control with a low value of ε , that is the traction control operates even when the difference between the speed of the two wheels is not too high, giving a “strong control.”

Even in this case, the effect of the traction control is evident. In case (C), the speed of the front wheel is similar to the speed of the rear wheel and consequently, the driver controls the motorcycle.

5. Conclusions

A new algorithm and its hardware implementation of traction control for supermotard or motocross are presented. A prototype has been realised and tested in a racing track. The experimental results show good performances of the system.

A more accurate tuning of the parameters of the controller should be done, depending on the style of drive of the driver and on the track and on the ground conditions, but the first results are positive.

The traction controller proposed can be applied to any existing motorcycle.

References

- [1] P. Kachroo and M. Tomizuka, “Vehicle traction control and its applications,” Tech. Rep. UCBITS- PRR-94-08, University of California, Berkeley, Calif, USA, March 1994.
- [2] K. Chun and M. Sunwoo, “Wheel slip tracking using moving sliding surface,” *International Journal of Automotive Technology*, vol. 5, no. 2, pp. 123–133, 2004.
- [3] R. Balakrishna and A. Ghosal, “Modeling of slip for wheeled mobile robots,” *IEEE Transactions on Robotics and Automation*, vol. 11, no. 1, pp. 126–132, 1995.
- [4] A. Bellini, A. Bemporad, E. Franchi, N. Manaresi, R. Rovatti, and G. Torricini, “Analog fuzzy implementation of a vehicle traction sliding-mode control,” in *Proceedings of the 29th International Symposium on Automotive Technology and Automation (ISATA '96)*, pp. 275–282, Florence, Italy, June 1996.
- [5] P. Kachroo and M. Tomizuka, “An adaptive sliding mode vehicle traction controller design,” in *Proceedings of the IEEE International Conference on Systems, Man and Cybernetics*, vol. 1, pp. 777–782, Vancouver, Canada, October 1995.
- [6] G. F. Mauer, “A fuzzy logic controller for an ABS braking system,” *IEEE Transactions on Fuzzy Systems*, vol. 3, no. 4, pp. 381–388, 1995.
- [7] H. S. Tan, *Adaptive and robust controls with application to vehicle traction control*, Ph.D. dissertation, University of California, Berkeley, Calif, USA, 1988.
- [8] H.-S. Tan and M. Tomizuka, “An adaptive sliding mode vehicle traction controller design,” in *Proceedings of the American Control Conference*, vol. 2, pp. 1856–1861, San Diego, Calif, USA, May 1990.
- [9] F. Borrelli, A. Bemporad, M. Fodor, and D. Hrovat, “An MPC/hybrid system approach to traction control,” *IEEE Transactions on Control Systems Technology*, vol. 14, no. 3, pp. 541–552, 2006.
- [10] K. Fujii and H. Fujimoto, “Traction control based on slip ratio estimation without detecting vehicle speed for electric vehicle,” in *Proceedings of the 4th Power Conversion Conference (PCC '07)*, pp. 688–693, Nagoya, Japan, April 2007.
- [11] M. Jalili-Kharaajoo and F. Besharati, “Sliding mode traction control of an electric vehicle with four separate wheel drives,” in *Proceedings of the IEEE Conference on Emerging Technologies and Factory Automation (ETFA '03)*, vol. 2, pp. 291–296, Lisbon, Portugal, September 2003.
- [12] J. Zhang, C. Yin, and J. Zhang, “Use of fuzzy controller for hybrid traction control system in hybrid electric vehicles,” in *Proceedings of the IEEE International Conference on Mechatronics and Automation (ICMA '06)*, pp. 1351–1356, Luoyang, China, June 2006.
- [13] V. D. Colli, F. Marignetti, R. Di Stefano, G. Tomassi, and M. Scarano, “Traction control for a PM axial-flux in-wheel motor,” in *Proceedings of the 12th International Power Electronics and Motion Control Conference (EPE-PEMC '07)*, pp. 1790–1795, Portoroz, Slovenia, August–September 2007.
- [14] Z. Ming and G. Ni, “A computationally intelligent methodologies and sliding mode control based traction control system for in-wheel driven EV,” in *Proceedings of the 5th CES/IEEE International Power Electronics and Motion Control Conference (IPEMC '07)*, vol. 2, pp. 1091–1095, Shanghai, China, August 2007.
- [15] M. Jalili-Kharaajoo and H. Rouhani, “Robust nonlinear control applied to traction control of electric vehicles,” in *Proceedings of the 10th IEEE International Conference on Electronics, Circuits and Systems (ICECS '03)*, vol. 1, pp. 392–395, Shadah, United Arab Emirates, December 2003.
- [16] <http://www.usautoparts.net/bmw>.
- [17] <http://www.webbikeworld.com/BMW-motorcycles>.
- [18] http://www.ducati.com/racing/00_home_racing/index.jhtml.